Journal of Fluorescence, Vol. 14, No. 3, May 2004 (©2004)

Heat Stress Induced Redistribution of Fluorescent Quantum Dots in Breast Tumor Cells

Olaf Minet,[1,3] Cathrin Dressler,[2] and Jürgen Beuthan[1]

Received August 31, 2003; revised January 10, 2004; accepted January 10, 2004

The probing of living cells in different colors over extended periods of time can be used to see the complicated processes that take place during carcinogenesis or heat stress, for example. Since most therapeutic laser tissue interactions are based on thermal effects a detailed characterization of thermal tissue damages in the cellular and sub-cellular levels is important. In order to study such microdosimetry laser-induced fluorescences of Quantum dots provide a suitable approach. Streptavidin conjugated Qdot™ 605 (Quantum Dot Corp., USA) were used in combination with the concanavalin A-biotin labeling system (Molecular Probes, NL) to observe membrane associated thermal lesions. Fluorescent Qdot conjugates are a promising alternative to organic dyes. The extinction coefficient of Qdot™ 605 streptavidin conjugate is 650,000 M^{-1} cm^{-1} at 600 nm. Red fluorescent Qdots™ 605 were selected because autofluorescence of cells in the red spectral range is not relevant. Fluorescence detection was performed with a confocal laser scan microscope LSM410 (Carl Zeiss, Germany). Breast cancer cells were used in the thermal stressing experiments performed at 40°C, 42°C, 45°C, 50°C or 56°C for 30 min, each. In this methodical approach Qdot mediated labeling of heat stressed cells were demonstrated to show alterations of plasma membrane organizations and integrities, respectively.

KEY WORDS: biomedical fluorescence; quantum dots; heat stress.

INTRODUCTION

The sciences of life want to probe living cells in full color over extended periods of time to see the rather complicated processes that take place during embryogenesis, carcinogenesis, and heat stress, for example. Existing fluorescence techniques use natural molecules like organic dyes and/or proteins or synthesized markers for Optical Molecular Imaging [1]. In this case light will be emitted over a wide spectral range, which means that the spectra will overlap and a differentiation of the dyes becomes harder the more dyes are involved. Inorganic semiconductor nanocrystals—called quantum dots—promise alternatives to the chemical fluorophores and visible fluorescent proteins.

Most therapeutic laser applications are based on thermal tissue effects. Depending on the medical indication thermal effects have to be generated by exact radiation parameters and appropriate laser specifications. Local tissue coagulations are induced with temperatures between 50°C and 100°C while surgical tissue ablations and hemostasis need to be performed at temperatures higher than 100°C [2]. Especially in the temperature range beneath 60°C therapeutic successes are predominantly influenced by the properties of a target tissue. At subcoagulating temperatures specific stress response mechanisms, including the complex reaction cascades during apoptosis, might be activated in single cells or confined tissue areas. The outcome always will be either cell survival or cell death [3]. Cellular genetics and phenomenologies of apoptotic and necrotic processes are completely different and should be strictly differentiated [4].

[1] Charité—Universitätsmedizin Berlin/Campus Benjamin Franklin, Institut für Medizinische Physik und Lasermedizin, Berlin, Germany.
[2] Laser-und Medizin-Technologie GmbH, Berlin Fabeckstraße 60-62, Berlin, Germany.
[3] To whom correspondence should be addressed. E-mail: minet@zedat.fu-berlin.de

1053-0509/04/0500-0241/0

Molecular genetics of cell stress responses have already been investigated in detail, mainly focusing on the so called heat-shock proteins [3,5] first described in 1962 by Ritossa [6]. Detailed knowledge of the phenomenology and pathophysiology of tissue specific heat induced stress reactions is not yet available. Only a few studies on selected tissue models have been published so far [e.g. 7–10]. Especially in the context of laser supported thermotherapies of tumors, like laser-induced interstitial thermotherapy [11–13], systematic studies exactly describing the dose-effect-relationships under application of clinically relevant laser parameters are necessary for the microdosimetric optimization of these interventions.

Heat induced stress reactions in diseased tissues or normal tissues adjacent to therapy targeted lesions are crucial factors of the laser therapeutic result. Active and passive cellular heat stress responses are dictated by the applied stress dose in a functional and phenomenological manner. Therefore, the microdosimetry of thermal laser therapies is a very important parameter [14].

A very suitable approach to study the phenomenon of heat stress in single cells is fluorescence microscopy, as one of the best established standard techniques in biomedical analytics and clinical diagnostics today. Fluorescence detection of specific structures and functions in cellular systems is provided by the tremendous variability of fluorescent probes and markers concerning target specificities as well as spectral properties [15–17]. After many different organic fluorescent dyes and GFP-based biosensors have been routinely used for fluorescent imaging of cells the luminescent quantum dots (QDots) have recently entered the field of bioanlytics.

QDots are semiconductor nanocrystals of small extension with special optical properties [18]. A structure consisting of some thousands of GaAs/AlGaAs atoms is as small as 4 nm in diameter, an In/P/AlGaAs structure even 3 nm. Therefore, such structures are frequently called zero-dimensional objects.

The order of magnitude of the electrons' de Broglie wavelength is similar to the size of quantum dot. The electron-hole pairs are located in the three spatial dimensions because the core is contained with a protective shell. This band gap has a higher electronic level which confines the electron-hole pairs. The fluorescence emission is confined to a narrow band of typically 20–30 nm full width at half maximum. The wavelength depends on the particle size, characteristically. For example, a QDot made from Cd/Se radiates green light of 520 nm or red light of 630 nm depending on whether the diameter is 3 nm or 5.5 nm. Quantum dots can be excited over a broad spectrum which means that a mixture of different kinds of QDots for multiple color imaging can be excited by a light source of a single wavelength between UV and red [19]. The inorganic shell of the QDots is of hydrophobic nature. Putting QDots to biology they must be prevented from coming into direct contact with water and must be prevented from quenching. Despite their name, QDots are about 10 times bigger than normal organic dyes, which can be a limit within cells. Furthermore, QDots must be non-toxic, should recognize selectively a specific target in cellular structure, and must not interfere with normal physiology. Various modifications of the outer surface have been successful. A courageous step toward solving this problem was done by encapsulating the QDots in micelles—a simple chemical aggregate made from two kinds of phospholipids [20]. The hydrophobic tails move away from the water, while the polar heads immerse themselves in aqueous environments. Qdots stay protected at the centre of the micelles. For example, QDots were injected into embryos of an African frog. Besides many other biological observations they have no detrimental effect on the embryonic development and were photostable *in vivo* for days (for example 14 h by a 50 mW, 488 nm laser [21]). Also QDot for targeting human tumors work in mice *in vivo*. The dots were conjugated to a peptide or antibody to recognize a specific cancer cell [20].

In general, the surface of the quantum dots can be conjugated with ligand specific molecules like antibodies, peptides or streptavidin for driving the biological activities [22–24]. Especially the streptavidin:biotin system is a widely used bridging tool in many labeling technologies. Since avidin and its derivatives selectively bind biotin and biotinylated proteins with high binding affinities (e.g. 10^{15}mol/L for streptavidin:biotin) they offer very versatile secondary fluorescent labels now extended by QDot-streptavidin conjugates [17,18,25]. The general structure of a QDot-streptavidin conjugate is illustrated in Fig. 1 [18].

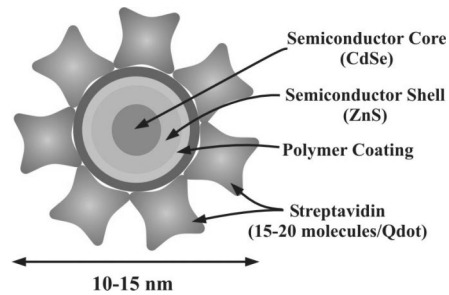

Fig. 1. Schematic of the overall structure a Qdot^{TM} streptavidin conjugate. The core consists of semiconductor material (CdSe), which has been coated with a semiconductor shell (ZnS). The polymer coating provided biochemical surface modification of the Qdot particle by direct coupling of the polymer to streptavidin [taken from Ref. 18].

This study was a methodical approach and intended to test the Qdot^{TM} streptavidin conjugate for investigating the microdosimetry of heat stress using mammary carcinoma cells (line MX1) as tumor model. Red fluorescent Qdots 605 were selected, because autofluorescence of cells in the red spectral range is very low. The extinction coefficient of Qdot^{TM} 605-streptavidin conjugate is 650,000 $M^{-1}cm^{-1}$ at 600 nm. Taking in mind the well known properties of the optical window in tissue optics, light with a wavelength in the visible or infrared range for excitation and fluorescence and the relatively high quantum efficiency of the QDots are a bonus when the light has to travel through bulk tissue.

Besides the complex network of metabolic processes the plasma membrane is the structure most prone to environmental stress like heat [26]. Therefore we chose glycoproteins as universal cellular plasma membrane target. Biotinylated concanavalin A (ConA) served as the targeting probe. ConA selectively binds to α-mannopyranosyl and α-glucopyranosyl residues in glycoproteins abundantly located in the glycocalyx of cellular plasma membranes [17,27]. This sandwich system was tested for its ability to support characterization of heat stress induced cellular changes using a confocal laser scan microscope (CLSM).

MATERIAL & METHODS

Cell Cultivation and Stressing

Human undifferentiated breast cancer cells of the line MX1 (Deutsches Krebsforschungszentrum, Germany) were employed as tissue model. Cells were maintained in RPMI 1640 medium supplemented with 20 mM HEPES, 10% (v/v) heat inactivated fetal calf serum, at 37°C and 5% CO_2 in humidified atmosphere. Cultures were dissociated with 0.05% trypsin-0.02% EDTA. 1% antibiotic-antimycotic solution (100 U/mL penicillin, 100 μg/mL streptomycin, 0.25 μg/mL amphotericin B; GIBCO^{TM} Invitrogen GmbH, Germany) was also added to the medium. All other culture medium components and solutions were purchased from Biochrom KG seromed, Germany. Experimental cells were grown in chamber slides (Nunc GmbH & Co. KG, Germany) until sub-confluent cell densities were achieved. Heat stress treatments were performed in a temperature-regulated water bath at the temperatures given with the results (40°C, 42°C, 45°C, 50°C, or 56°C) for 30 min, each. Immediately after heat stressing cells were submitted to further experimental processing.

Quantum Dot Labeling

Cells were rinsed in cold phosphate buffered saline (PBS) and internal biotin was blocked by incubating cells in 50 μg/mL Avidin (Sigma Aldrich Chem., Germany) in PBS (30 min, 37°C). Cells were triple rinsed in cold PBS before application of 250 μg/mL concanavalin A-biotin-conjugate (Molecular Probes, NL) in PBS (30 min, 37°C). Streptavidin conjugated Qdot^{TM} 605 (Quantum Dot Corp., USA) nanocrystals were used to label cell bound ConA mediated by biotin:streptavidin bridging. Qdot-conjugate stock solution was diluted 1:10 in incubation buffer supplied by the manufacturer 20 min prior to application. The final concentration of 0.1 μmolar was obtained by mixing equal volumes of PBS and Qdot solution. After 30 min incubation the cells were rinsed three times and micrographed in PBS. This labeling protocol is mainly based on the manufacturer's recommendations [18,25], alterations have been mentioned above.

Confocal Laser Scan Microscopy

Fluorescence emission measurements were performed with a LSM 410 (Carl Zeiss, Germany). The wavelengths 488 nm and 568 nm of an external argon-krypton laser (Spectra Physics GmbH, Germany) were used for exciting fluorescence signals. Emission signals were detected using a dichroitic beam splitter FT 580 and a long-pass filter LP 590. A scan resolution of 3×8 bits/0.5 s (512×512 pixels) was applied for each fluorescence image. All measurements were performed under confocal conditions (pinhole 20) at room temperature.

Cell Viability Screening via Colorimetric Microassay

Prior to QDot labeling experiments the impact of heat stressing on cell viability was screened with a colorimetric micro assay. AlamarBlue^{TM} (BIOSOURCE International Inc., USA) was used as metabolic reduction–oxidation indicator exhibiting a blue color in the native oxidized form or a red color after metabolic reduction. MX1 cells were seeded into flat-bottomed 96-well microtitre plates (Nunc GmbH & Co. KG, Germany) at 10^4 cells/well and incubated for 20 h under physiological growth conditions permitting the cells to adhere to the substrate inside the cavitities with culture volumes of 200 μL/well. Then the cells were heat stressed as described before and submitted to the AlamarBlue^{TM} cell activity assay according to the manufacturer's recommendations [28]. After 4 h reincubation under physiological conditions the reduction reaction was stopped by refrigerating the microplates (4°C) until measurement. Absorption photometric evaluations of the plates were performed using a Dynex MRX II microplate reader combined with the Revelation G 3.2 software (Dynex Technologies, USA) at 570 nm (measurement wavelength) and 630 nm (reference wavelength). Temperature dependant cell activities were quantified in

correlation with control cells (100% cell viability) and negative controls (no cells).

Quantum dots themselves are not toxic. The toxicity of the buffer was measured (data not shown), but did not induce any structural changes in cells. Functional defects were not investigated. Since Qdot labeling and microscopic viewing of specimens were performed after heat stress interventions, measured fluorescence intensities are not correlated to known temperature effects of QDots themselves.

RESULTS & DISCUSSION

Heat stresses at temperatures of 40°C or 42°C for 30 min, each did not impair cellular activities compared with the unstressed control cells as shown by the AlamarBlue™ based micro assay (Fig. 2). On the other hand cells stressed at 40°C were activated and exhibited a 20% higher viability than the control. Only stress doses above 42°C decreased cellular viabilities with increasing temperatures as expected. After treating cells at 56°C a minor metabolic rest activity below 20% was detected.

These data correlated well with the fluorescence micrographs measured by LSM. As expected control cells (37°C) and cells stressed at 40°C or 42°C exhibited regular growth conformations with intact tissue integrities and tissue specific cell morphologies. The QDot fluorescence was mainly restricted to the external leaflets of plasma membranes and intercellular areas (Fig. 3A–C). Nevertheless the fluorescence intensity distributions were irregular as illustrated by the 3D intensity profiles. When stressing

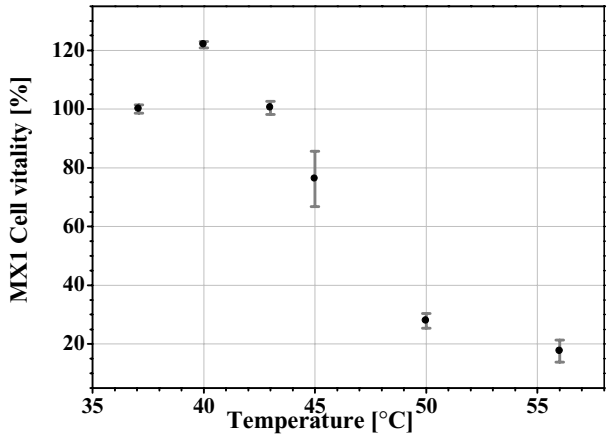

Fig. 2. Screening the metabolic activities of breast cancer cells (MX1) after heat stress using the AlamarBlue™-microassay. 48 measurements were averaged for every experimental group. The distributions of single measurements are indicated. Measurement wavelength: 570 nm reference wavelength: 630 nm.

was performed at 45°C or 50°C (Fig. 3D+E) the cells were smaller and rounder than in the control group (Fig. 3A). Also the tissue integrities were clearly dispersed indicating active cellular stress responses during heat treatments. This effect was more pronounced in the 50°C group than in the 45°C group. Here the 3D profiles exhibited more regular fluorescence intensity distributions than under minor stress conditions (40°C and 42°C). At the same time QDot fluorescence was also detected at the cytoplasmic leaflets of plasma membranes supporting the presumption that plasma membranes were reorganized and permitted QDot conjugates to enter the cells. Nuclei in these cells were still intact and exhibited no fluorescence while in the cells severely damaged at 56°C structural integrities of the plasma membranes and nuclear membranes were destroyed and fluorescence accumulated intracellularly penetrating the nuclear compartments (Fig. 3F). At 56°C a more or less spontaneous necrosis was induced since the cells did not exhibit round shapes indicating that heat stress at 56°C was too severe to allow active stress responses. The phenomena described are illustrated in more detail by the intensity profiles in Fig. 3. If the stress responses observed after temperatures of 45°C or 50°C were applied could be correlated with apoptotic processes is yet unknown since so far apoptosis has not been investigated on MX1 cells under the stress conditions described here.

Our results correspond well with the data published by Hymer *et al.* [10] where temperatures higher than 45°C were found to injure cell membranes in human skin cells. Although heat treatments were performed with a time regimen (1–300 s) different from the one used in our study, it can generally be concluded that the highly conserved membrane structure of animal cells is destabilized when faced with temperatures of 45°C or higher. Cell specific and individual differences in heat sensitivities obviously are most pronounced in this temperature range. This statement is supported by the comparatively large mean square deviations (m.s.d.) of the cell viability at 45°C as shown in Fig. 2, while the viabilities in the cell groups stressed at 40°C, 42°C, 50°C, and 56°C exhibited much smaller m.s.d.

The experimental protocol recommended by the manufacturer [18] has been modified in the way that the QDot labeling reaction was performed in a 50% PBS and 50% incubation buffer (provided by manufacturer) solution and not in 100% incubation buffer. In a previous experiment when QDot labeling was performed in 100% incubation buffer cells obviously were intoxicated and the formation of vacuoles was induced as shown in Fig. 4. Since the original incubation buffer is basic (pH 8.3) it employs non physiological conditions during incubations. Therefore the experimental conditions and special

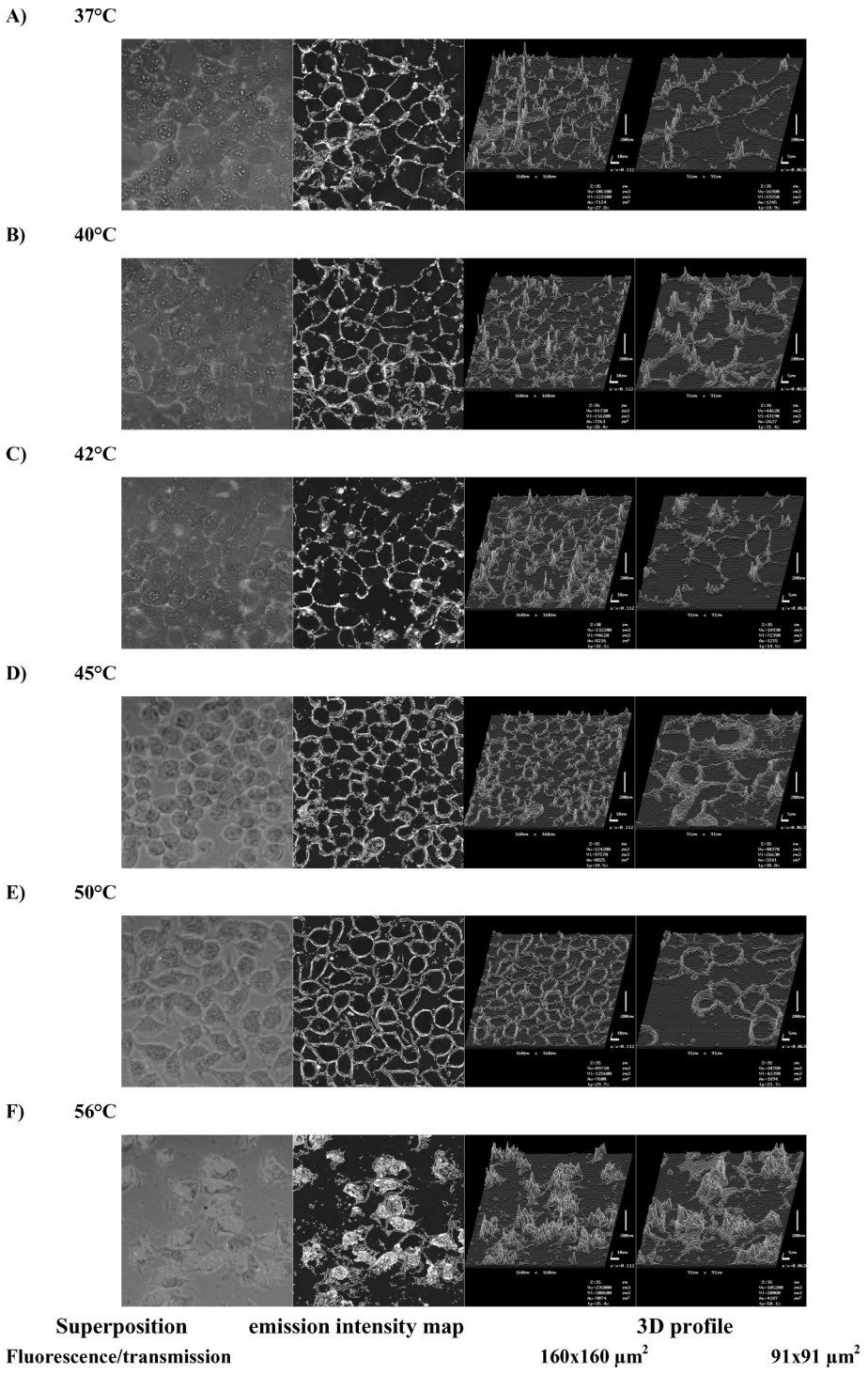

Fig. 3. Laser scan microscopy of MX1 cancer cells labeled with quantum dots. Panel A shows control cells, heat stressed cells (30 min each) are shown in the panels B–F. All panels include the superposition of fluorescence micrograph and transmission (left), the emission intensity map (centre), and the 3D signal intensity profiles (both right with different resolution). Fluorescence emissions were excited with the laser wavelengths 488 nm and 568 nm and emission signals were detected in the spectral range above 590 nm (FT 580, LP 590). For the fluorescence intensity imaging the integration time was 8 s/scan and 16 s/scan for $160 \times 160\ \mu m^2$ and $91 \times 91\ \mu m^2$, resp.

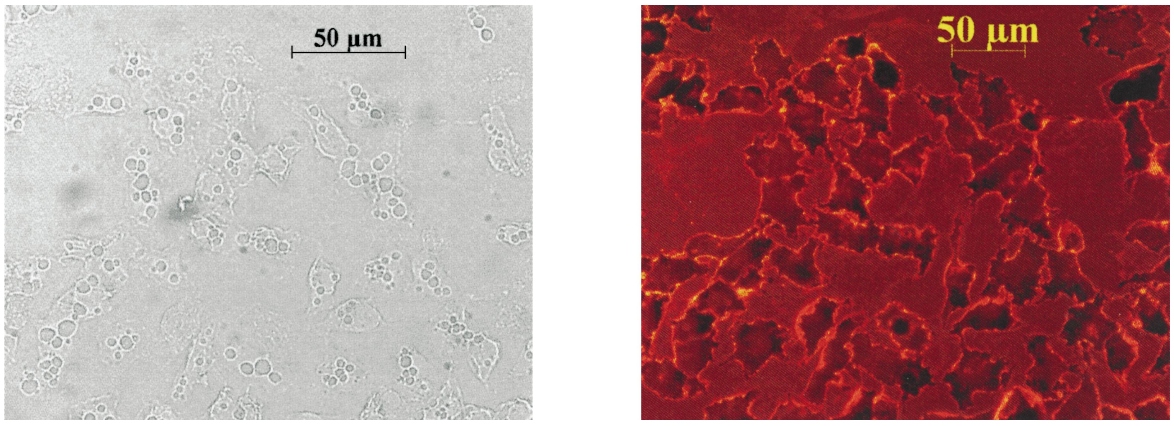

Fig. 4. Light (left) and fluorescence (right) microscopy (Axioplan 2, Carl Zeiss, Germany) of MX1 cancer cells labeled with quantum dots in 100% incubation buffer provided by the manufacturer [18]. After a 30 min incubation period at room temperature the cells exhibited vacuoles.

preparation of the cells under investigation should be optimized for every cell type prior to QDot labeling procedures. Valuable information on the preconditioning of labeling experiments using QDots are given in Ref. 18, 21–24.

Under the experimental conditions applied in this study the phenomenology of cellular response to heat stress were outlined. General cytomorphological features, mainly cell shape, tissue conformation, membrane integrity, as well as the organization of nuclei were visualized after QDot fluorescence detection. Investigations on specific sub-cellular features especially protein functions and their molecular genetic basis will have to use target specific probes and appropriate detection methods, respectively. In general, QDots show a much brighter fluorescence light due to higher quantum yield in comparison to organic fluorescent dyes. But future availability of different QDot conjugated probes will benefit bioanalytical studies on the dynamics of stress responses induced by physiological or environmental stress factors. The benefits of QDot labeling will be accomplished by minimal spectral overlaps in multicolor labeling applications and long-term photostability. This will be associated with reduced technological requirements for fluorescence detection systems. The employment of QDot labeling of specific targets will be advantageous for real-time monitoring of various intracellular processes. Especially the use of QDot encoded multiplexed assays and high-throughput analyses of genes and proteins are of interest [19,29].

Also in the field of single molecule detection and spectroscopy QDots are promising alternatives to fluorescent biomolecules because of their high photoluminescence yields [30]. Highly sensitive techniques like scanning near-field optical microscopy (SNOM) providing high lateral resolutions could detect single QDots and might favor the localization and quantification of specific targets or low-abundance biomolecules on cell membranes or various sub-cellular organelles or selected structures.

Our study only focused on spontaneous stress responses while long-term impacts on cell-survival, apoptotic pathways or genetic over expression rates were not included. Especially cancer cells are in a general state of genetic instability eventually causing various sub-clones to be resistant to internal and external stress factors [31–33]. This implies the necessity for studying phenotypes and genotypes of heat stress responses in different tissue species in detail. Further results dealing with these subjects will enhance laser-assisted hyperthermia treatments.

REFERENCES

1. O. Minet, J. Beuthan, K. Licha, and C. Mahnke (2002). in R. Kraayenhof, A. J. W. G. Visser, H. C. Gerritsen (Ed.), *Fluorescence Spectroscopy, Imaging and Probes* (Springer Series on Fluorescence Methods and Applications), Vol. 2, Springer, New York, pp. 349–360.
2. O. Minet, K. Dörschel, and G. Mueller (2004). Lasers in biology and medicine. in Landolt-Börnstein (Ed.), *Laser Applications*, Vol. VIII/1c, Springer, New York, pp. 279–310.
3. D. L. Vaux (2002). Apoptosis and toxicology—what relevance? *Toxicology* **181**–**182**, 3–7.
4. S. Y. Proskuryakov, A. G. Konoplyannikov, and V. L. Gabai (2003). *Exp. Cell Res.* **283**, 1–16.
5. S. L. Rutherford (2003). *Nat. Rev. Genet*. **4**, 263–274.
6. F. M. Ritossa (1962). *Drosophila*. *Experimenta* **18**, 571-573.
7. F. Macouillard-Poulletier de Gannes, N. Leducq, P. Diolez, F. Belloc, M. Merle, P. Canioni, and P.-J. Voisin (2000). *Neurochem. Int.* **36**, 233–241.
8. A. Yagui-Beltran, A. L. Graig, L. Lawrie, D. Thompson, S. Pospisilova, D. Johnston, N. Kernohan, D. Hopwood, J. F. Dillon, and T. R. Hupp (2001). *Eur. J. Biochem*. **268**, 5343–5355.
9. J. Jakubowicz-Gil, J. Rzymowska, and A. Gawron (2002). Quercetin, apoptosis, heat shock. *Biochem. Pharmacol*. **64**, 1591–1595.
10. http://www.ntar3.sr.unh.edu/download/191/paper191.doc

11. S. Jacques, C. Newman, and X. Y. He (1991). *Am. Soc. Mech. Eng.* **189**, 71–73.
12. B. Gewiese, J. Beuthan, F. Fobbe, D. Stiller, G. Müller, J. Böse-Landgraf, K. J. Wolf, and M. Deimling (1994). *Invest. Radiol.* **29**, 345–351.
13. S. H. Diaz, J. S. Nelson, and B. J. F. Wong (2002). *Phys. Med. Biol.* **48**, 19–29.
14. A. J. Welch and M. J. C. van Germert (1995). *Optical-Thermal Response of Laser-Irradiated Tissue*, Plenum, New York.
15. M. P. Oksvold, E. Skarpen, J. Widerberg, and H. S. Huitfeldt (2002). *J. Histochem. Cytochem.* **50**, 289–303.
16. D. J. Stephens and V. J. Allen (2003). *Science* **300**, 82–86.
17. http://www.probes.com/handbook
18. http://www.qdots.com
19. W. C. W. Chan, D. J. Maxwell, X. Gao, R. E. Bailey, M. Han, and S. Nie (2002). *Curr. Opin. Biotechnol.* **13**, 40–46.
20. B. Dubertret, P. Skourides, D. J. Norris, V. Noireaux, A. H. Brivanlou, and A. Libchaber (2002). *Science* **298**, 1759–1762.
21. J. K. Jaiswal, H. Mattoussi, J. M. Mauro, and S. M. Simon (2003). *Nat. Biotechnol.* **21**, 47–51.
22. E. R. Goldman, G. P. Anderson, P. T. Tran, H. Matoussi, P. T. Charles, and J. M. Mauro (2002). *Anal. Chem.* **74**, 841–847.
23. M. E. Akerman, W. C. W. Chan, P. Laakkonen, S. N. Bhatia, and E. Ruoslahti (2002). *Proc. Natl. Acad. Sci.* **99**, 12617–12621.
24. X. Wu, H. Liu, J. Liu, K. N. Haley, J. A. Treadway, J. P. Larson, N. Ge, F. Peale, and M. P. Bruchez (2003). *Nat. Biotechnol.* **21**, 41–46.
25. P. S. Stayton, K. E. Nelson, T. C. McDevitt, V. Bulmus, T. Shimooji, Z. Ding, and A. S. Hoffman (1999). *Biomol. Eng.* **16**, 93–99.
26. J. C. Chato and R. C. Lee (1998). *Ann. N. Y. Acad. Sci.* **858**, 1–20.
27. H. Rüdiger and H.-J. Gabius (2001). *Glycoconj. J.* **18**, 589–613.
28. http://www.biosource.com/content/literatureContent/PDFs/alamarbluebooklet.pdf
29. H. Xu, M. Y. Sha, E. Y. Wong, J. Uphoff, Y. Xu, J. A. Treadway, A. Truong, E. O'Brien, S. Asquith, M. Stubbins, N. K. Spurr, E. H. Lai, and W. Mahoney (2003). *Nucleic Acids Res.* **31**, No.8 *e*43.
30. K. Ikeda, K. Matsuda, H. Saito, K. Nishi, and T. Saiki (2001). *J. Microsc.* **202**, 209–211.
31. N. Narita, I. Noda, T. Ohtsubo, S. Fujeda, M. Tokuriki, T. Saito, and H. Saito (2002). *Int. J. Radiat. Oncol. Biol. Phys.* **53**, 190–196.
32. X. Zhang, Y. Li, Q. Huang, H. Wang, B. Yan, M. W. Dewhirst, and C. Y. Li (2003). *Clin. Cancer Res.* **9**, 1155–1160.
33. E. Zeise and L. Rensing (2002). *Int. J. Hyperthermia* **18**, 344–360.